Title

Link Lifetime asa Function of Node Mobility in MANETs with Restricted Mobility:Modeling and Applications

Author

Garcia-Luna-Aceves, J.J.

Publication Date

2007-04-16

Peer reviewed

Link Lifetime as a Function of Node Mobility in MANETs with Restricted Mobility: Modeling and Applications

Xianren Wu[1], Hamid R. Sadjadpour[1] and J.J. Garcia-Luna-Aceves[1,2]
[1]University of California at Santa Cruz, Santa Cruz, CA 95064, USA, email: {wuxr,hamid}@soe.ucsc.edu
[2]Palo Alto Research Center, 3333 Coyote Hill Road, Palo Alto, CA 94304, USA, email: jj@soe.ucsc.edu

***Abstract*— We present statistical models to accurately evaluate the distribution of the lifetime of a wireless link in a mobile ad hoc network (MANET) in which nodes move randomly within constrained areas. We show that link lifetime can be computed through a two-state Markov model and further apply the computed statistics to the optimization of segmentation schemes of information stream. Summarizing all these results, we further provide comprehensive analysis on throughput, delay, and storage requirements for MANETs with restricted node mobility.**

I. Introduction

Mobility brings fundamental changes to the performance and design of all aspects of protocol stacks in MANETs. Understanding the statistics of link lifetime is crucial for accurate analysis of MANET parameters and protocols. For example, the performance of routing protocols in MANET exhibits direct relationship to the mean value of link lifetime [1]. Interestingly, as critical as link lifetime is for the performance of the protocol stack in MANET, no analytical model of link lifetime exists to accurately characterize it as a function of node mobility, which is a defining attribute of MANETs! As a result, link lifetime in MANET has been analyzed mostly through simulations, and analytical modeling of channel access and routing protocols for MANETs have not represented the temporal nature of MANET links accurately. Similarly, most studies of routing-protocol performance have relied exclusively on simulations, or had to use limited models of link availability, to address the dynamics of paths impacting routing protocols.

This paper provides the most accurate analytical model of link lifetime in MANETs to date, and characterizes link lifetime as a function of node mobility. The importance of this model is twofold. First, it enables answering many questions regarding fundamental tradeoffs in throughput, delay and storage requirements in MANETs, as well as the relationship between many protocol-design choices (e.g., packet length) and network dynamics (e.g., how long links last in a MANET). Second, it enables the development of analytical models for channel access and routing schemes by allowing such protocols to use link lifetime expressions that are very accurate with respect to simulations based on widely-used mobility models.

Recently, Samar and Wicker [2], [3] pioneered the work of analytical evaluation of link dynamics. They further provided good insights on the importance of an analytical formulation of link dynamics to the optimization of the protocol design. However, Samar and Wicker assume that communicating nodes maintain constant speed and direction in order to evaluate the distribution of link lifetime. This simplification overlooks the case in which either of the communicating nodes changes its speed or direction while the nodes are in transmission range of each other. As a result, the results predicted by Samar and Wicker's model could deviate from reality greatly, being overly conservative and underestimating the distribution of link lifetime [2], [3], especially when the ratio R/v between the radius of the communication range R to the node speed v becomes large, such that nodes are likely to change their velocity and direction during an exchange.

Another contribution of the paper is to provide the first comprehensive coverage of MANETs with restricted mobility, where each node moves within a constrained area. These networks play an important role in the real world, where nodes usually travel only a portion of the entire network. As published in the *information assurance framework* [4] from National Security Agency, such networks represent the more realistic scenarios for tactical users, especially for the users deployed in the division and rear area. The only prior work that we are aware is given by Groenevelt et al. in [5]. It covers delay aspects of such networks but for the case of one dimensional restricted mobility. For this reason, we strive in this paper to provide the first thorough analysis (to the best of authors' knowledge) of two-dimensional restricted mobility networks on link dynamics, optimal segmentation of information stream, and throughput, delay, and storage tradeoffs.

The paper is organized as follows. Section II describes system models including network and mobility models in the paper. Section III presents the proposed two-state Markov model and results on link lifetime, along with simulation results for model validation. Section IV uses the derived statistics of link lifetime in section III for the problem of optimal segmentation of information stream. Section V provides a thorough analysis of throughput, delay and storage capacity of a MANET with restricted mobility, followed by concluding remarks in section VI.

II. System Model

In many tactical applications [4], nodes of a MANET traverse only a small portion of the entire area covered by the network. We consider a square or rectangular area partitioned into squarelets similar to prior analytical models of MANETs and as depicted in Fig. 1. The entire network is divided into multiple squarelets, which we call *cells*, and each cell is of size $L \times L$.

This work was supported in part by the US Army Research Office under grants W911NF-05-1-0246 and by the Baskin Chair of Computer Engineering. Opinion, interpretations, conclusions and recommendations are those of the authors and are not necessarily endorsed by the Department of Defense.

Communication between nodes in neighboring cells is allowed around their cell boundaries and all nodes transmit at uniform power. According to the protocol model [6], the allowable communication region should be deliberately designed to avoid excessive interference to nearby cells and to satisfy protocol model. Referring to the design in [7], a feasible solution is to choose circular regions centered at cell boundaries, as depicted in Fig. 1.

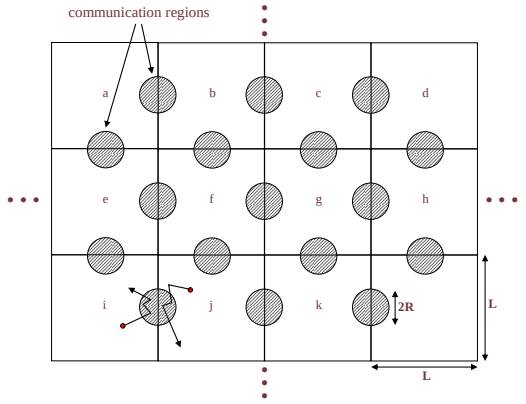

Fig. 1. Model of network structure

A typical communication session between two nodes involves several control and data packet transmissions. Depending on the protocol, nodes may be required to transmit beacons to their neighbors to synchronize their clocks for a variety of reasons (e.g., power management, frequency hopping). Nodes can find out about each other's presence by means of such beacons, or by the reception of other types of signaling packets (e.g., HELLO messages). Once a transmitter knows about the existence of a receiver, it can send data packets, which are typically acknowledged one by one, and the MAC protocol attempts to reduce or avoid those cases in which more than one transmitter sends data packets around a given receiver, which typically causes the loss of all such packets at the receiver. To simplify our modeling of link lifetimes, we assume that the proper mechanisms are in place for neighboring nodes to find each other, and that all transmissions of data packets are successful as long as they do not last beyond the lifetime of the wireless link between transmitter and receiver. Relaxing this simplifying assumption is the subject of future work, as it involves the modeling of explicit medium access control schemes (e.g., [8]).

Nodes are mobile and distributed over these cells. Nodes move according to the widely-used random direction mobility model (RDMM) [9], [10], [11], [12], [13], which improves on the random waypoint mobility model to have a uniform stationary spacial node distribution. Nodes movements are independent and identically distributed (iid) and can be described by a continuous-time stochastic process. The continuous movement of nodes is divided into mobility epochs during which a node moves at constant velocity, i.e., fixed speed and direction. But the speed and direction varies from epoch to epoch. The time duration of epochs is denoted by a random variable τ, assumed to be exponentially distributed with parameter λ_m. Its complementary cumulative distribution function (CCDF) $F_m(\tau)$ can be written as [11].

$$F_m(\tau) = exp(-\lambda_m \tau) \tag{1}$$

The direction during each epoch is assumed to be uniformly distributed over $[0, 2\pi)$ and the speed of each epoch is uniformly distributed over $[v_{min}, v_{max}]$, where v_{min}, v_{max} specify the minimum and maximum speed of nodes respectively. Speed, direction and epoch time are mutually uncorrelated and independent over epochs.

The movement of each node is restricted into the cell where it is initially located. Each source node randomly chooses its destination and in most cases, the source and destination nodes are not within the same cell. As a result, most data traffic need to travel across cells and links over neighboring cells are focal points for such networks. The analysis of this paper is focused on inter-cell links but our analysis can be also extended to intra-cell links or nodes with unrestricted mobility.

III. Link Lifetime

A bidirectional link exists between two nodes if they are within communication range of each other. In this paper, we do not consider unidirectional links, given that the vast majority of channel access and routing protocols use only bidirectional links for their operation. Hence, we will refer to bidirectional links simply as links for the rest of this paper.

When a data packet starts at time t_0, positions of nodes (e.g. nodes m_a and m_b) during communication session could be anywhere inside communication range. The location of nodes should follow the stationary spacial distribution of the RDMM and thus can be considered as uniformly distributed. Let B ($bits/s$) be the transmission rate of a data packet, L_p be the length of the data packet, and $t_0 + T_a$ (or $t_0 + T_b$) denotes the moment a node m_a (or m_b) is moving out of communication range. A packet can be successfully transferred only if nodes m_a and m_b stay within communication range during the entire communication session, that is,

$$L_p/B \leq T_L \tag{2}$$

$$T_L = min(T_a, T_b). \tag{3}$$

T_L is the link lifetime (LLT) which is the maximum possible data transfer duration. Statistically, T_a and T_b specify the distribution of residence time that measures the duration of the time, for either nodes m_a or m_b, starting from a random location inside the communication region with equal probability and continuously stay inside the communication region before finally moving out of it.

Given that the motions of nodes are iid, the distribution of T_a and T_b is the same. We call it the *single-node link lifetime* (S-LLT) distribution. Furthermore, its complementary cumulative distribution function (CCDF) is denoted by $F_S(t)$, i.e., $F_S(t) = P(T_a \geq t) = P(T_b \geq t)$. Clearly, we can compute the CCDF $F_L(t)$ as

$$F_L(t) = F_S^2(t). \tag{4}$$

And the link outage probability P_{L_p} associated with a particular packet length L_p can be evaluated as

$$P_{L_p} = P(T_L \leq \frac{L_p}{B}) = 1 - F_L(\frac{L_p}{B}). \tag{5}$$

A. Single-Node Link Lifetime (S-LLT)

From the above, it follows that the essence of modeling link dynamics in MANETs consists of evaluating the distribution of S-LLT, because it reflects the link dynamics resulting from the motions of nodes. S-LLT measures the duration of time for a node to continuously stay inside the communication range of another node. In our model, this range is a circle.

We also know that the movement of nodes consists of a sequence of mobility epochs. Let A_s be the starting point of current mobility epoch and its position will be uniformly distributed over communication circle [11]. The end point of the current epoch is denoted by A_d, and A_d may be anywhere in the cell, i.e., inside or out of the communication circle. In the case that A_d is located inside the communication circle, it serves as the starting point (i.e., new A_s) for the next epoch and the whole process is repeated. In the evaluation of S-LLT, the repeating procedure ends when the final A_d is out of the communication region.

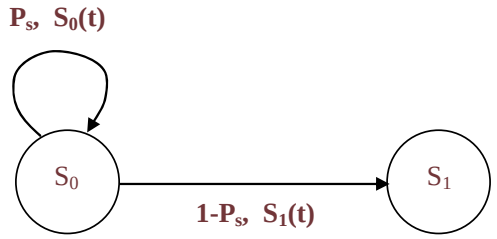

Fig. 2. Two-state Markovian model for S-LLT evaluation

As illustrated in Fig. 2, the procedure for evaluating the S-LLT can be modeled as a two-state Markovian process. The sojourn state S_0 represents the scenario where the end point A_d of current epoch is located inside the communication circle, while the departing state S_1 refers to the complementary scenario where A_d will be out of communication region. Compared to the model by Samar and Wicker [2], [3], in which only the last scenario (i.e., state S_1) is considered, the two-state Markovian model reflects the motion of nodes more accurately, which naturally expects better results in evaluating link dynamics.

Let P_s be the *residence probability*, which denotes the probability that A_d is located inside the communication region. The probability distribution function (PDF) $S_0(t)$ specifies the distribution of sojourn time of mobility epochs when a node stays in state S_0. Correspondingly, the PDF $S_1(t)$ is used to measure the distribution of departing times when nodes move out of communication regions and switch to the state S_1.

Before eventually moving out of the communication region, i.e., being switched to the departing state S_1, nodes may stay at the residence state S_0 multiple times. Let N_i be the integer variable counting the number of times for a node to remain in state S_0, and $\{S_{0,0}, \ldots, S_{0,N_i-1}\}$ be the associated random variables that specify the duration of time of mobility epochs for each return.

Clearly, $\{S_{0,0}, \ldots, S_{0,N_i-1}\}$ are random variables of the same distribution but correlated. However, to make our problem more tractable, we assume that $\{S_{0,0}, \ldots, S_{0,N_i-1}\}$ are statistically i.i.d random variables of distribution $S_0(t)$. Our simplifying assumption deviates the final result slightly from the real situation when the residence probability becomes larger. However, as we will see later, our model still provides good approximations, even with a large residence probability.

We define S_1 as the random variable measuring the departing time of distribution $S_1(t)$. Simply, one can evaluate conditional single-node link lifetime $T_S(N_i)$ as

$$T_S(N_i) = \sum_{i=0}^{N_i-1} S_{0,i} + S_1 \quad (6)$$

$$P(N_i = K) = P_s^K \quad (7)$$

The characteristic function $U_{T_S}(\theta)$ for the S-LLT T_S can now be evaluated as

$$\begin{aligned} U_{T_S}(\theta) &= E(e^{j\theta T_S}) \\ &= \sum_{k=0}^{\infty} E(e^{j\theta(\sum_{i=0}^{k-1} S_{0,i}+S_1)})P(N_i = k) \\ &= \sum_{k=0}^{\infty} U_1(\theta)U_0(\theta)^k P_s^k \\ &= \frac{U_1(\theta)}{1 - U_0(\theta)P_s} \end{aligned} \quad (8)$$

where $U_0(\theta)$ and $U_1(\theta)$ are the characteristic functions of $S_0(t)$ and $S_1(t)$ respectively.

When the radio range is pretty small compared to the cell size and nodes' speed, A_d will be mostly located outside of the communication region. Consequently, one will have $P_s \ll 1$. Given that $U_0(\theta)$ is the characteristic function of $S_0(t)$, one has $|U_0(\theta)| \leq 1$. Finally, it is clear that $U_0(\theta)P_s \ll 1$. Therefore, Eq. (8) can be approximated as

$$U_{T_S}(\theta) \approx U_1(\theta) \quad (9)$$

For clarification purposes, we call Eq. (8) as the Exact S-LLT (ES-LLT), which is based on the two-state Markovian model. The approximation in Eq. (9) is called Approximated S-LLT (AS-LLT), and it reflects the scenario considered by Samar and Wicker [2], [3].As we will see later, the analytical expression of AS-LLT is the same to the expression in [2], [3], except for a normalization factor.

To evaluate the S-LLT T_S, we need to evaluate P_s, $S_0(t)$, and $S_1(t)$, which we do next.

Let z_d denote the least distance to be traveled by node to move out of the communication circle, starting from the position A_s with the direction and speed v being kept unchanged. A graphical illustration of z_d is presented in Fig. 8. The probability P_s can now be evaluated through z_d as

$$P_s = E_v(P_s(v)) \quad (10)$$

$$\begin{aligned} P_s(v) &= \int_{z_d} P(\tau \leq \frac{z_d}{v})p(z_d)dz_d \\ &= \int_{z_d} (1 - F_m(\frac{z_d}{v}))p(z_d)dz_d \\ &= \int_{z_d} (1 - exp(-\lambda_m z_d/v))p(z_d)dz_d \end{aligned} \quad (11)$$

where $P_s(v)$ is the conditional probability of P_s on v. $p(z_d)$ is PDF of z_d and from Appendix, we know that it can be calculated as

$$p(z_d) = \begin{cases} \frac{2}{\pi R^2}\sqrt{R^2 - (\frac{z_d}{2})^2}, & \text{for } 0 \le z_d \le 2R \\ 0, & \text{elsewhere} \end{cases} \quad (12)$$

where R specifies the radius of the communication circle.

$S_0(t)$ is the PDF of the time duration for nodes to return to the state S_0. Conditioning on speed v and assuming that the starting time is at time 0, $S(t)$ is the probability of the node changing its velocity at time t on condition that A_d is located inside the communication circle. Hence,

$$\begin{aligned} S_0(t) &= E_v(S_0(t|v)) \quad (13) \\ S_0(t|v) &= \frac{1}{P_s}P(t=\tau, z_d \ge v\tau|v) \\ &= \frac{1}{P_s}\lambda_m e^{-\lambda_m t}\int_{vt}^{2R} p(z_d)dz_d \\ &= \begin{cases} \frac{2\lambda_m e^{-\lambda_m t}}{P_s \pi R^2}\int_{vt}^{2R}\sqrt{R^2-(\frac{x}{2})^2}dx, & 0 \le t \le \frac{2R}{v} \\ 0, & \text{elsewhere} \end{cases} \\ &= \begin{cases} \frac{4\lambda_m e^{-\lambda_m t}}{\pi P_s}\int_{\frac{vt}{2R}}^{1}\sqrt{1-x^2}dx, & 0 \le t \le \frac{2R}{v} \\ 0, & \text{elsewhere} \end{cases} \quad (14) \end{aligned}$$

where $S_0(t|v)$ is the conditional PDF on v.

$S_1(t)$ can be evaluated in much the same way as we have done for $S_0(t)$. Conditioning on speed v and assuming that the starting time is at time 0, $S_1(t)$ is simply the probability of the node moving out of the communication circle at time t with velocity being kept constant. Hence,

$$\begin{aligned} S_1(t) &= E_v(S_1(t|v)) \quad (15) \\ S_1(t|v) &= \frac{1}{1-P_s}P(t=\frac{z_d}{v},\ z_d \le v\tau|v) \\ &= \frac{1}{1-P_s}P(\tau \ge t)p(z_d = vt)(vt)' \\ &= \begin{cases} \frac{2e^{-\lambda_m t}}{(1-P_s)\pi R^2}v\sqrt{R^2-(\frac{vt}{2})^2}, & 0 \le t \le \frac{2R}{v} \\ 0, & \text{elsewhere} \end{cases} \\ &= \begin{cases} \frac{4e^{-\lambda_m t}}{\pi(1-P_s)}\frac{v}{2R}\sqrt{1-(\frac{vt}{2R})^2}, & 0 \le t \le \frac{2R}{v} \\ 0, & \text{elsewhere} \end{cases} \quad (16) \end{aligned}$$

where $S_1(t|v)$ is the conditional PDF on v. A detailed examination of Eq.(15) reveals that it shares the same core analytical expression of link lifetime distribution of Eq. (15) in [3], with the only exception that a normalization factor $e^{-\lambda_m t}/(1-P_s)$ accounts for the probability of nodes leaving for state S_1. It implies that AS-LLT formula, solely relying on $S_1(t)$, gives the same link lifetime distribution as in [3].

B. Model Validations

In the simulation, there are a total of 100 nodes randomly placed for each $1000m \times 1000m$ square cell. Each node has the same transmit power and two profiles of the radio transmission range are chosen for simulation. Both are within the coverage of IEEE 802.11 PHY layer and they are $\{200m, 100m\}$. After initial placement, nodes keep moving continuously according to the RDMM model. The mobility parameter λ_m is chosen to be $\lambda_m = 4$ and three different speeds are simulated $v \in \{1, 10, 20\}(m/s)$, from pedestrian speed to normal vehicle speed. Combining the power profile and velocity profile, six different scenarios are simulated $\{I : (200m, 1m/s); II : (100m, 1m/s); III : (200m, 10m/s); IV : (100m, 10m/s); V : (200m, 20m/s); VI : (100m, 20m/s)\}$.

Nodes are randomly activated to randomly choose destination node for data transmission. The traffic of activated nodes are supplied from a CBR source with a packet rate $0.5p/s$. Given that the choice of specific MAC layer and routing protocol may affect the results, we assume perfect MAC and routing, rendering zero delays or losses due to such functionality, enabling the simulation to capture statistics solely due to mobility.

Table I describes the residence probability P_s for all six scenarios. As shown in Table I, the residence probability increases with the relative radius ReR $\frac{R}{v}$, indicating that it is more likely for nodes with larger ReR to stay inside the communication circle.

It is worthy of noting that the two-phase Markov model is a general model able to evaluate other networks with the two building blocks $S_0(t)$ and $S_1(t)$ adapted for the specific network and mobility models. We have applied the two-phase model to model random waypoint mobility model and obtained similar results. For the reason of space limitations, we only provide the results of RDMM model here. Fig. (3) and (4) present the results of link lifetime with ES-LLT and AS-LLT formula for both intra-cell and inter-cell links. The results clearly confirm that the two-state Markovian model is a powerful tool to accurately model link dynamics of link lifetime distribution as a function of node mobility. It can be observed that the ES-LLT formula, obtained from the Markovian model, shows good match with the simulations in all scenarios. On the other hand, the AS-LLT formula with the simplified assumptions corresponding to the model by Samar and Wicker [2], [3] gives good approximation to the simulations only for small values of ReR $\frac{R}{v}$ and greatly deviates from the simulations when ReR $\frac{R}{v}$ becomes large, i.e., larger residence probability P_s and larger possibility for nodes to stay inside communication circle. Furthermore, it is also clear that lifetime of inter-cell links is much shorter than intra-cell links, indicating the bottleneck effect from inter-cell links on network throughput.

TABLE I
RESIDENCE PROBABILITY P_s.

$R\ (m)$	$v\ (m/s)$		
	1	10	20
100	0.09	0.01	0.005
200	0.17	0.02	0.01

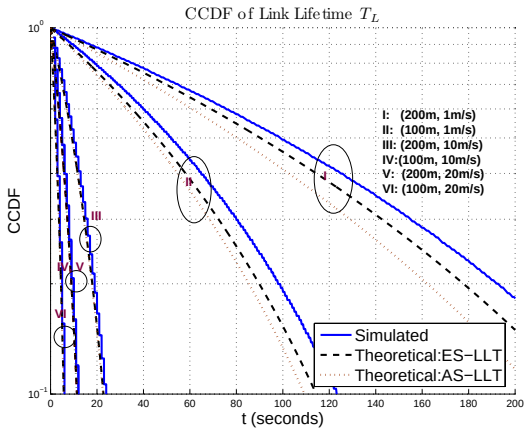

Fig. 3. Link Lifetime T_L (inter-cell): Simulated, ES-LLT(Markovian), AS-LLT.

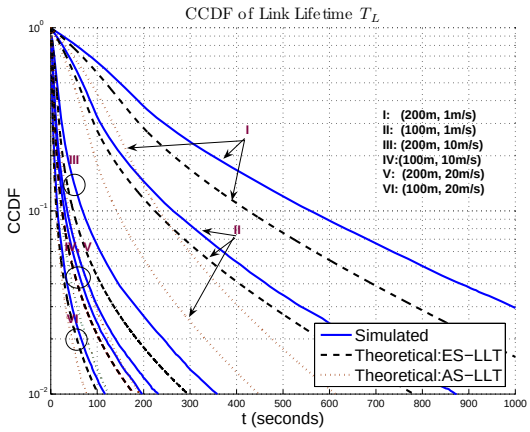

Fig. 4. Link Lifetime T_L (intra-cell): Simulated, ES-LLT(Markovian), AS-LLT..

IV. Segmentation Schemes and Their Optimization

In wireless communication, source bit-stream usually needs to be segmented into a sequence of fix-length information data packets for transmission. These information data packets will be further processed (e.g. channel encoding) to fit into various transmission schemes. Given that nodes move in a MANET, the data transfer can be broken if one of the two nodes moves out of the communication circle. Within this highly dynamic environment, it is quite important to design segmentation schemes or use information data packet lengths that maximize throughput. If a data-packet length is too long, frequent link breaks could lead to significant packet dropout during the transfer. On the other hand, if data packet length is too short, the overhead from sub layer processing could significantly reduce the effective throughput. Judicious design of segmentation scheme as a function of link dynamics can be of great importance in maximizing throughput of MANETs. However, this problem remain almost undeveloped since its solution necessitates exact knowledge of statistics of link lifetime. With the computed CCDF in section III, we are now able to provide segmentation schemes optimized on various systematic constraints.

When the length of data packets is constant, it is fairly natural to ask what will be the optimal packet length. For every packet length L_p, we know that there is an associated link outage probability P_{L_p} specifying the probability of link breach during packet transfer. Every dropped packet during link outage needs to be retransmitted and therefore reduces the effective throughput.

One segmentation scheme is to simply choose the maximum possible packet length L_0 that satisfies a pre-defined link outage probability requirement. We term this scheme as link outage priority design (LOPD) and it can be described as

$$L_0 = max_{L_p}\, P_{L_p} \leq \omega_p \tag{17}$$

where ω_p is a constant to specify the link dropout probability requirement.

Alternatively, we can use a cost function $C(L_p, P_{L_p})$ that incorporates the negative effect from the packet retransmission into evaluating the effective throughput $T(L_p)$ for a specific packet length L_p. Further optimizing the effective throughput $T(L_p)$ gives the optimal packet length L_0. Consequently, this segmentation scheme is termed as link throughput priority design (LTPD).

In the LTPD design, when the packet length is L_p, we can describe the effective throughput $T(L_p)$ function as

$$T(L_p) = (1 - P_{L_p}) \cdot L_p - C(L_p, P_{L_p}) \cdot P_{L_p} \cdot L_p \tag{18}$$

The optimal packet length L_0 will be the one that maximizes the effective throughput

$$L_0 = max_{L_p}\, T(L_p) \tag{19}$$

Normally, P_{L_p} is a monotonically decreasing function. When the cost function is chosen to be a constant penalty value, i.e., $C(L_p, P_{L_p}) = C$, by taking the derivative with respect to L_p, the optimal packet length L_0 is the value satisfying

$$1 - (1 + C)P_{L_0} = (1 + C)L_0 \left.\frac{dP_{L_p}}{dL_p}\right|_{L_p = L_0}. \tag{20}$$

In Fig. 5, we exploit the application of link lifetime distribution to the optimization of segmentation scheme using the same examples of the previous section. The cost function for our example of LTPD design is chosen as a constant penalty value 2 (i.e., $C(L_p, P_{L_p}) = 2$) and the effective throughput $T(L_p)$ is computed for every L_p and drawn for all three methods: Simulation, ES-LLT (Markovian model), and AS-LLT. As expected, ES-LLT approximates simulation very well, while AS-LLT tends to conservatively underestimate the effective throughput for larger ReR. In addition, all curves of the effective throughput (either Simulation, ES-LLT, or AS-LLT formula) are convex functions with numerical solution readily available.

The optimized solutions $\frac{L_0}{B}$ of both LOPD and LTPD protocols on information segmentation are illustrated in Fig. 6. In the simulation, the link outage tolerance of LOPD design is set to be $\omega_p = 0.1$, i.e., the maximum link outage probability should be less than 10%. Two key observations should be made: (1) For both LTPD and LOPD designs, the ES-LLT (Markovian

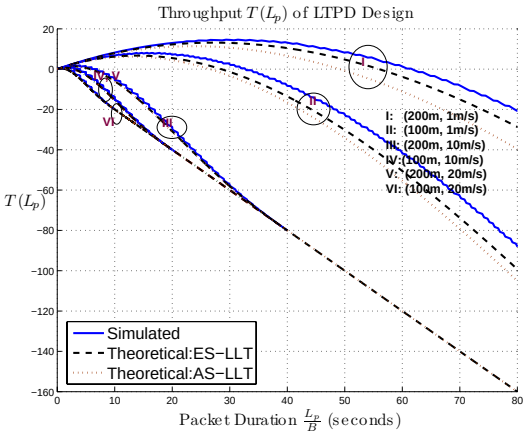

Fig. 5. LTPD Design.

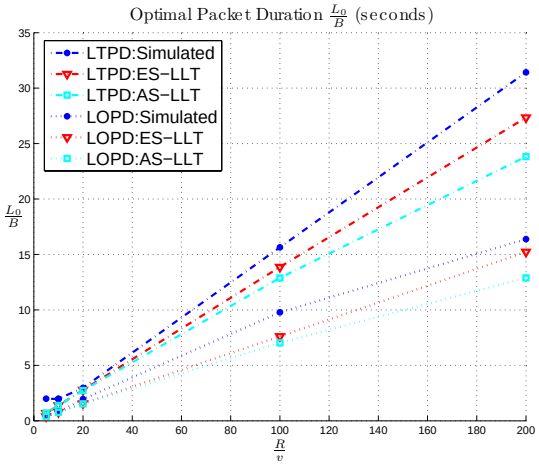

Fig. 6. Optimal Packet Duration $\frac{L_0}{B}$.

model) approaches the simulated optimal solution well, and signifies substantial improvement of throughput over the AS-LLT model ([2], [3]); and (2) LTPD design suggests a balanced design between longer packet and larger retransmission rate to offer higher throughput over LOPD design. LOPD design, on the other hand, tends to be more conservative on the throughput but resulting in less packet retransmission.

Another important observation from Fig. 6 is that the optimal packet length designs, obtained from either the simulation or Markovian ES-LLT formula, exhibit linear proportion to the ReR value $\frac{R}{v}$. It suggests that mathematically, the optimal information segmentation should follow the rule [1]

$$\frac{L_0}{B} = \Theta(\frac{R}{v}). \tag{21}$$

V. Analysis of Throughput, Average Delay and Storage

A. Throughput

We consider store-and-forward scheme similar to the one in MANETs with unlimited mobility [14], [15]. Source node splits information stream to relay nodes in its neighbor cells. Each relay stores information in the queue and delivers information from the queue only when it meets another relay nodes or the destination node in another cell. By doing it, usage of relays is minimized to improve the overall throughput. We also assume that every relay node maintains a separate queue for each source-destination pair and the queue is served in a First-Come-First-Serve (FCFS) manner. Because all cells resemble each other and nodes have iid movements, it is clear that all such queues are similar. Furthermore, we adopt a conservative scenario in which only one node per cell can act as the relay node of a specific route for later delay analysis. In reality, every node can act as a relay, which leads to less delay but a much more complex network of queues.

[1]We recall the following notation: (i) $f(n) = O(g(n))$ means that there exists a positive constant c and integer N such that $f(n) \leq cg(n)$ for $n > N$. (ii) $f(n) = o(g(n))$ means that $\lim_{n\to\infty} f(n)/g(n) = 0$. (iii) $f(n) = \Omega(g(n))$ means that $g(n) = O(f(n))$. (iv) $f(n) = \omega(g(n))$ means that $g(n) = o(f(n))$. (v) $f(n) = \Theta(g(n)$ means that there exist positive constants c_1, c_2 and M, such that $0 \leq c_1 g(n) \leq f(n) \leq c_2 g(n)\ \forall n > M$.

To facilitate our analysis, distribution of link interarrival time (LIT) for inter-cell links is summarized in the following Theorem and the proof is provided in Appendix.

Theorem 1: Let nodes A and B are moving independently of each other in two adjacent square cells of size $L \times L$. And their movement follow the RDMM model and are of average speed $E(v)$. Then LIT of such inter-cell links between nodes is approximately exponentially distributed with parameter λ_I, where λ_I and the mean time of I is given by

$$\lambda_I = \frac{\pi^2 \cdot E(v) \cdot R^3}{2L^4} \tag{22}$$

$$E(I) \approx \frac{2L^4}{\pi^2 \cdot E(v) \cdot R^3} \tag{23}$$

For every cell, there should be at least one node inside the cell in order to maintain the connectivity of the network. Let $a(n) = \frac{L^2}{A_N}$ be the fractional cell size, where A_N is the overall size of the network. The connectivity requirement necessitates [16] that only when $a(n) \geq \frac{2log(n)}{n}$, each cell has at least one node *with high probability (whp)*, i.e., with probability $\geq 1 - \frac{1}{n}$. In this case, each cell will have $\Theta(na(n))$ nodes inside *whp* [16].

Recall that for inter-cell links, the size L_0 of a data packet should be chosen as $L_0 = \Theta(\frac{R \cdot B}{E(v)})$. With reference to Theorem 1, on average, every time duration of $E(I) = \Theta(\frac{L^4}{E(v) \cdot R^3})$ could have one data packet transfered. Accordingly, link throughput T_0 for one such pair of nodes can be computed as

$$T_0 = \frac{L_0}{I} = \Theta(\frac{R^4 B}{L^4}) \tag{24}$$

Normally, R is chosen on the same order of L, i.e., $\frac{R}{L} = \Theta(1)$. The above equation will be reduced to be $T_0 = \Theta(B) = c_0$, where c_0 is a constant. Furthermore, from the connectivity constraint, there is at least one such link available for each node.

Due to limited mobility and transmission range, each packet needs to travel via multiple relays from source to destination following the path close to the straight line linking source and destination. Let the straight line connecting source with destination in the snapshot of initial network deployment be denoted

as S-D line. Clearly, a source transmits data to its destination by multiple relays along the adjacent cells lying on its S-D line.

Let K be the average number of source-destination (S-D) lines passing through every cell and each source generates traffic $\Lambda(n)\ bits/s$. To ensure that all required traffic is carried and recall that on average there are $\Theta(na(n))$ nodes in every cell, we need that

$$K \cdot \Lambda(n) \leq T_0 \cdot \Theta(na(n)) \Rightarrow \Lambda(n) = O(\frac{na(n)}{K}) \quad (25)$$

For every cell, the following lemma gives the number K of S-D lines passing through it.

Lemma 1: The number K of S-D lines passing through any cell is $\Theta(n\sqrt{a(n)})$, *whp*.

The proof of this lemma follows the proof of Lemma 3 in [16], because the S-D lines are determined from the initial network deployment, which is a snapshot of MANET and can also be treated as one configuration of a static wireless network.

The above analysis leads to the following conclusion on the throughput $\Lambda(n)$.

Theorem 2: For cell partitioned network with restricted mobility, we have $\Lambda(n) = O(\sqrt{a(n)})$ for generic mobility models. In particular, for a connected network *whp*, $\Lambda(n) = O(\sqrt{\frac{log(n)}{n}})$.

B. Delay & Storage

Most packets need to travel across several cells before reaching their destinations and, therefore, must be stored in the queue of relay nodes. Consider an S-D queue at relay node m_r, a packet arrives when node m_r and the previous relay node (or the source node) simultaneously come into the communication region; a packet departs when m_r meets another relay node (or the destination node) in the communication region. Both the inter-arrival time and the inter-departure time are of the same order as link interarrival time (LIT). Since LIT can be characterized as exponentially distributed, each queue is characterized by a Poisson arrival process with exponential service time, thus being a M/M/1-FCFS queue.

For each S-D pair, queues at relay nodes construct a M/M/1-FCFS feedforward tandem network[2]. An important property of such a M/M/1-FCFS feedforward tandem network is the *Jackson's theorem* (see [17], page 150), i.e., if the tandem network with exponential service time is driven by a Poisson arrival process, every queue in the tandem network behaves as if it were an independent M/M/1-FCFS queue and thus can be analyzed individually. Recall the following properties for a M/M/1-FCFS queue (see [17], chapter 3) in the following lemma.

Lemma 2: Consider a discrete M/M/1-FCFS queue. Let $1-\epsilon$ be the *traffic intensity* and λ be the exponential *service rate* of the queue, the average delay is given by

$$E(D) = \frac{1}{\lambda\epsilon} = \Theta(\frac{1}{\lambda}) \quad (26)$$

[2]For delay to be finite, the arrival rate must be strictly less than the service rate but in this case, symmetric movements lead to a fully loaded tandem queue. To avoid this, we assume that if the available throughput is $\Lambda(n)$, each source generates traffic at a rate $(1-\epsilon)\Lambda(n)$, for some $\epsilon > 0$.

Furthermore, the mean and variance of the occupancy of the queue N_q is,

$$E(N_q) = \frac{1-\epsilon}{\epsilon} = \Theta(1) \quad (27)$$

$$Var(N_q) = \frac{1-\epsilon}{\epsilon^2} = \Theta(1) \quad (28)$$

Without loss of generality, we can assume that the overall size of network is of unit area to analyze the network. In this case, we will have $A_N = 1$ and $L = \sqrt{a(n)}$. The average distance between S-D pairs is given by $\Theta(1)$ and the average number of hops for each packet is $\Theta(1/\sqrt{a(n)})$. Recall that every relay node carries information for $\Theta(n\sqrt{a(n)})$ S-D pairs and the service rate of each queue from LIT is $\lambda = \Theta(\frac{E(v)}{\sqrt{a(n)}})$[3]. *Jackson's theorem* indicates that the delay for each S-D pair is the summation of delays occurred at relay nodes.

We can summarize the network performance in terms of average delay and storage in the following theorem.

Theorem 3: The average packet delay in a cell-partitioned network with restricted mobility and RDMM mobility models is given by

$$D(n) = \overbrace{\Theta(\frac{1}{\sqrt{a(n)}})}^{\#\ of\ hops} \cdot \overbrace{\Theta(\frac{\sqrt{a(n)}}{E(v)})}^{delay\ at\ each\ hop} = \Theta(\frac{1}{E(v)}) \quad (29)$$

and the average information bit delay $D_b(n)$ is

$$D_b(n) = \frac{D(n)}{\Theta(\frac{RB}{E(v)})} = \Theta(\frac{1}{RB}) \quad (30)$$

Furthermore, the mean and variance of the packet occupancy (i.e., storage requirement) is given by

$$E(N_p) = Var(N_p) = \Theta(n\sqrt{a(n)}) \quad (31)$$

and the corresponding bit storage requirement N_b is

$$E(N_b) = Var(N_b) = \Theta(n\sqrt{a(n)}) \cdot \Theta(\frac{RB}{E(v)}) \quad (32)$$

VI. CONCLUSIONS

We have presented an analytical framework for the characterization of link lifetime in MANETs with restricted mobility. Given the existence of prior attempts to incorporate link lifetime in the modeling of routing and clustering schemes [18], [19], [20], we believe that this new framework will find widespread use by researchers interested in the analytical modeling and optimization of channel access and routing protocols in MANETs.

We also apply the computed statistics from our framework to address the optimization of segmentation schemes as a function of link dynamics in a MANET. The optimized solutions

[3]It can be obtained by substituting $\frac{R}{L} = \Theta(1)$ and $L = \sqrt{a(n)}$ into Eq. (22).

obtained from the proposed analytical framework show a substantial improvement on network throughput. Eventually, we summarize all these results to provide the first comprehensive analysis on throughput, average delay and storage requirements for MANETs with restricted mobility. For future research efforts, we would like to consider another important aspect of network - modeling of network lifetime and exploit its statistics to the application of performance analysis of routing protocols.

ACKNOWLEDGEMENT

The authors would like to thank Dr. Robin Groenevelt and Prof. Philippe Nain of INRIA university for their kind help on providing the simulation environment.

REFERENCES

[1] F. Bai, N. Sadagopan, and A. Helmy. Important: A framework to systematically analyze the impact of mobility on performance of routing protocols for adhoc networks. In *22th Infocom*, pages 825 – 835, San Francisco, 2003.
[2] P. Samar and S. B. Wicker. On the behavior of communication links of a node in a multi-hop mobile environment. In *ACM MobiHoc 04*, pages 148–156, 2004.
[3] P. Samar and S. B. Wicker. Link dynamics and protocol design in a multi-hop mobile environment. *IEEE Transactions on Mobile Computing*, to appear.
[4] National Security Agency. *Assurance Technical Framework*, chapter 9. 3.1 edition, 2002.
[5] R. B. Groenevelt, E. Altman, and P. Nain. Relaying in mobile ad hoc networks: The brownian motion mobility model. *Springer Journal of Wireless Networks (WINET)*, 12:561–571, October 2006.
[6] P. Gupta and P. R. Kumar. The capacity of wireless networks. *IEEE Trans. on Information Theory*, 46(2):388–404, March 2000.
[7] R. M. Moraes, H. R. Sadjadpour, and J.J. Garcia-Luna-Aceves. Mobility-capacity-delay trade-off in wireless ad-hoc networks. *Elsevier*, July 2005.
[8] M. Carvalho and J.J. Garcia-Luna-Aceves. A scalable model for channel access protocols in multihop ad hoc networks. In *Proc. ACM Mobicom 2004*, Philadelphia, Pennsylvania, September 2004.
[9] S. Jiang, D. He, and J. Rao. A prediction-based link availability estimation for mobile ad hoc networks. In *IEEE Infocom*, pages 1745–1752, April 2001.
[10] S. Jiang, D. He, and J. Rao. A prediction-based link availability estimation for routing metrics in manets. *IEEE/ACM Transactions on Networking*, 13(6):1302–1312, December 2005.
[11] A. B. McDonald and T. F. Znati. A mobility-based framework for adaptive clustering in wireless ad hoc networks. *IEEE Journal on Selected Areas in Communications*, 17(8):1466–1487, August 1999.
[12] C. Bettstetter. Mobility modeling in wireless network: categorization, smooth movement and border effects. *ACM Mobile Computing and Communication Review*, 5:55–67, January 2001.
[13] R. Guerin. Channel occupancy time distribution in a cellular ratio system. *IEEE Trans. on Vehicular Technology*, VT-35(3):89–99, August 1987.
[14] M. Grossglauser and D. Tse. Mobility increases the capacity of ad-hoc wireless network. In *Proc. of Twentieth Annual Joint Conference of the IEEE Computer and Communications Societies*, volume 3, pages 1360–1369, April 2001.
[15] M. Grossglauser and D. Tse. Mobility increases the capacity of adhoc wireless networks. *IEEE/ACM Transactions on Networking*, 10(4):477–486, August 2002.
[16] A. E. Gammal, J. Mammen, B. Prabhaker, and D. Shah. Throughput-delay trade-off in wireless networks. In *Infocom*, volume 1, pages 464–475, 2004.
[17] L. Kleinrock. *Queuing Systems, Volume 1: Theory*. John Wiley & Sons, Inc, 1975.
[18] N. Sadagopan et al. Paths: Analysis of path duration statistics and their impact on reactive manet routing protocols. In *ACM MobiHoc 03*, Annapolis, MD, June 2003.
[19] A. Tsirigos and Z.J. Haas. Analysis of multipath routing - part i: The effect on the packet delivery ratio. *IEEE Transactions on Wireless Communications*, 3(1):138–146, January 2004.
[20] D. Turgut et al. Longevity of routes in mobile ad hoc networks. In *VTC' 01*, Greece, May 2001.
[21] N. Bansal and Z. Liu. Capacity, delay and mobility in wireless ad-hoc networks. In *Infocom*, 2003.
[22] D. Hong and S. S. Rappaport. Traffic model and performance analysis for cellular mobile radio telephone systems with prioritized and non prioritized handoff procedures. *IEEE Transactions on Vehicular Technology*, 35(3):77–92, August 1986.

APPENDIX

A. Proof of Theorem 1

The proof proceeds by modeling the meeting of two nodes in the communication region as a geometric variable with some probability p of success and then taking the limit to derive the exponential distribution. The probability p will depend on the speeds and the positions of the two nodes. The probability p is obtained through summarizing the three exclusive scenarios analyzed below.

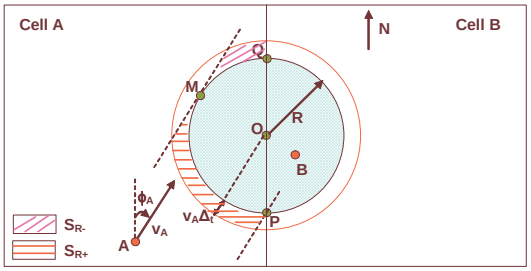

Fig. 7. Illustration of the first scenario.

We first consider the case where node B is inside the communication region within the time duration $[t, t+\Delta_t)$, while node A moves into the communication region with some probability p_1. Because Δ_t is fairly small, we can assume that there is no change of directions within the duration Δ_t. The probability p_B that node B is located inside the communication region at time t can be obtained from the stationary distribution,

$$p_B = \int\int_{S_B} \zeta(x,y)dxdy \tag{33}$$

where $\zeta(x,y)$ stands for the stationary spatial nodes' distribution and S_B (or S_A) denotes the semicircle of the communication region in the cell B (or cell A). Meanwhile, we can also have similar definition of p_A. Because nodes are moving independently, the probability p_1 will be the product of p_B and p_{S_A}. p_{S_A} represents the probability of events that node A moves into the communication region within time frame $[t, t+\Delta_t)$. It can be noted that we have neglected the probability of node B moving out of the communication region within the time frame $[t, t+\Delta_t)$. In fact, the probability is on the same order of the third scenario and can be expressed as $o(\Delta_t)$.

Clearly, the probability p_{S_A} varies with the initial location, speed v_A and direction ϕ_A of node A at time t. Without loss of generality, we can assume $\phi_A \in [0, \pi]$ in our analysis. Conditioning on v_A and ϕ_A, within time duration $[t, t+\Delta_t)$, node A can at most travel towards the center point O for a distance of $v_A\Delta_t$. It implies that node A should be located inside the ring area in *cell A* in Fig. 7 for it to move into the communication region within time duration $[t, t+\Delta_t)$.

To construct the ring area, we first draw two lines parallel to the direction ϕ_A. One line passes point Q, while another line is a tangential line with respect to the circular communication region at point M. For every point on $arcA$, we can draw a line passing through the point (termed as *cross* point) and in the meanwhile being parallel to the direction ϕ_A. One outmost point (called *verge* point) on the verge of the ring area can then be determined by looking for the point lying on the line in the meanwhile of distance $v_A\Delta_t$ to *cross* point. The *verge* point should be inside *cell A* while outside the communication region. To ensure that node A can move into the contact region S_A within time duration $[t, t+\Delta_t)$ with velocity v_A and direction ϕ_A, the location of node A at time t should be within the shaded area S_{R+}, i.e., the intersection area formed by the ring and the two parallel lines along direction ϕ_A in Fig. 7.

Let $arcPM$ be the arc from point P to point M on the circumference. Conditioning on v_A and ϕ_A, the probability $p_{S_{R+}}$ for node A moving into the communication can now be computed as

$$\begin{aligned} p_{S_{R+}|\{v_A,\phi_A\}} &= \int\int_{S_{R+}} \zeta(x,y)dxdy \\ &\approx v_A\cdot\Delta_t\cdot p_{arcPM} \end{aligned} \tag{34}$$

where $p_{arcPM} = \int\int_{arcPM}\zeta(x,y)dxdy$. Consider the supplementary scenario where node A is of the same location and speed at time t but moving at direction $\phi_A-\pi$. Obviously, node A should now be within the supplementary area S_{R-} in Fig. 7. Let $arcQM$ be the arc from point Q to M on the circumference. The complementary probability $p_{S_{R-}}$can now be obtained as

$$\begin{aligned} p_{S_{R-}|\{v_A,\phi_A\}} &= \int\int_{S_{R-}} \zeta(x,y)dxdy \\ &\approx v_A\cdot\Delta_t\cdot p_{arcQM} \end{aligned} \tag{35}$$

where $p_{arcQM} = \int\int_{arcQM}\zeta(x,y)dxdy$.

Noting that $arcA = arcPM + arcQM$, where $arcA$ (or $arcB$) is the circumference of the communication circle inside *cell A* (or *cell B*). We will have $p_{arcA} = p_{arcPM}+p_{arcQM}$, and averaging over all possible v_A and ϕ_A's, the probability p_{S_A} is given by

$$\begin{aligned} p_{S_A} &= E_{v_A}\{\frac{1}{2\pi}\int_0^\pi (p_{S_{R+}|\{v_A,\phi_A\}}+p_{S_{R-}|\{v_A,\phi_A\}})d\phi_A\} \\ &= E_{v_A}\{\frac{1}{2\pi}v_A\cdot\Delta_t\cdot\int_0^\pi (p_{arcPM}+p_{arcQM})d\phi_A\} \\ &= E_{v_A}\{v_A\cdot\Delta_t\cdot p_{arcA}\cdot\frac{1}{2\pi}\int_0^\pi 1\ d\phi_A\} \\ &= \frac{E(v_A)}{2}\cdot\Delta_t\cdot p_{arcA} \end{aligned} \tag{36}$$

The above leads to

$$p_1 = p_{S_A}\cdot p_B = \frac{E(v_A)}{2}\cdot\Delta_t\cdot p_{arcA}\cdot p_B \tag{37}$$

The next scenario for our proof consists of symmetric scenario where node A stays inside the communication region within the time duration $[t, t+\Delta_t)$, while node B is going to move into the communication region by some probability p_2. Following similar derivations and analysis, p_2 can be calculated as

$$p_2 = \frac{E(v_B)}{2}\cdot\Delta_t\cdot p_{arcB}\cdot p_A \tag{38}$$

The last scenario we need to consider for our proof is the case where both node A and node B are located outside the communication region at time t but are going to move into the communication region within time duration $[t, t+\Delta_t)$. In contrast to the two prior scenarios in which one node is within the communication region while another one is located within the ring area at time t, in this case both nodes should be located within their respective ring area at time t.

It should be noted that the analytical procedure through geometric-variable analysis in the above scenarios can also be applied to analyze this scenario with minor modifications expected. For the purpose of succinctness, we will not elaborate on the derivations and our analysis shows that the probability p_3 for this case can be summarized as

$$\begin{aligned} p_3 &= E\{v_A\cdot v_B\cdot\Delta_t^2\cdot p_{arcA}\cdot p_{arcB} \\ &\quad\cdot(\frac{1}{2\pi})^2\int_0^\pi\int_0^\pi 1\ d\phi_A d\phi_B\} \\ &= \frac{E(v_A)E(v_B)}{4}\cdot\Delta_t^2\cdot p_{arcA}\cdot p_{arcB} \\ &= o(\Delta_t) \end{aligned} \tag{39}$$

Summarizing all three scenarios, we obtain that the probability p is given by

$$\begin{aligned} p &= p_1+p_2+p_3 \\ &= \frac{1}{2}\cdot\Delta_t\cdot(E(v_A)\cdot p_{arcA}\cdot p_B \\ &\quad +E(v_B)\cdot p_{arcB}\cdot p_A)+o(\Delta_t) \end{aligned} \tag{40}$$

Taking the limit $\Delta_t\to 0$ gives an exponential distribution with parameter $\lambda_F \approx \frac{E(v_A)\cdot p_{arcA}\cdot p_B+E(v_B)\cdot p_{arcB}\cdot p_A}{2}$.

Till now, we have arrived at a proof of Theorem 1 on general mobility models. For RDMM model, it should be noted that the stationary spatial nodes' distribution is uniform, i.e., $\zeta(x,y) = 1/L^2$ [12], [21]. It in turn gives $p_{arcA} = p_{arcB} = \int\int_{arcA}\zeta(x,y)dxdy = \frac{\pi\cdot R}{L^2}$ and $p_A = p_B = \int\int_{S_A}\zeta(x,y)dxdy = \frac{\pi\cdot R^2}{2L^2}$. By substituting these equations into the above proof, Theorem 1 follows.

B. Distribution of z_d

From Section III-A, we know that z_d denotes the least distance to be traveled by node to move out of the communication circle, if the direction and speed of node are kept unchanged. The current position of the node is random and uniformly distributed inside the communication circle. As illustrated in Fig. 8, there are two cases to be considered in calculating the z_d: 1) z_d is the distance along the direction of current velocity (i.e., line $A_s\to B$); 2) z_d is comprised of two

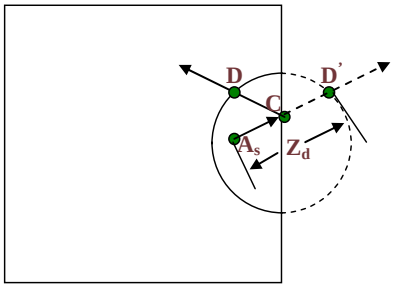

Fig. 8. Graphical Illustration of z_d.

parts, where the first part is the distance along current direction to hit the cell boundary and the other part is along the reflected direction starting from the reflecting point (i.e., lines $A_s \rightarrow C, C \rightarrow D$).

In the second case, we can consider as if the node travels across the boundary along the previous direction without being reflected back. Taking the above example, it is equivalent to say that $A_s \rightarrow C, C \rightarrow D$ can be substituted by $A_s \rightarrow D^{'}$. In this way, z_d can be calculated as if it were moving in a complete circle.

We have thus successfully translated the problem of calculating z_d into a similar problem discussed by Hong and Rappaport [22] of calculating the distance traveled by a mobile user in its originated cell before finally being switched to adjacent cell for handoff. Following similar derivations as in [22], the distribution of z_d is given by

$$p(z_d) = \begin{cases} \frac{2}{\pi R^2}\sqrt{R^2 - (\frac{z_d}{2})^2}, & \text{for } 0 \leq z_d \leq 2R \\ 0, & \text{elsewhere} \end{cases} \tag{41}$$

where R is the radius of the communication circle.